**Structural Engineering and Mechanics**, *Vol. 65, No. 5 (2018) 535-546*
DOI: https://doi.org/10.12989/sem.2018.65.5.535


# Analytical and numerical studies on hollow core slabs strengthened with hybrid FRP and overlay techniques

Pradeep Kankeri[1a], S. Suriya Prakash*[2] and Sameer Kumar Sarma Pachalla[3b]

[1]*Department of Civil Engineering, Vardhaman College of Engineering, Hyderabad, India*
[2]*Department of Civil Engineering, Indian Institute of Technology Hyderabad, India*
[3]*Department of Civil Engineering, Mahindra Ecole Centrale, Hyderabad, India*

*(Received April 1, 2017, Revised December 5, 2017, Accepted January 3, 2018)*

**Abstract.** The objective of this study is to understand the behaviour of hollow core slabs strengthened with FRP and hybrid techniques through numerical and analytical studies. Different strengthening techniques considered in this study are (i) External Bonding (EB) of Carbon Fiber Reinforced Polymer (CFRP) laminates, (ii) Near Surface Mounting (NSM) of CFRP laminates, (iii) Bonded Overlay (BO) using concrete layer, and (iv) hybrid strengthening which is a combination of bonded overlay and NSM or EB. In the numerical studies, three-dimensional Finite Element (FE) models of hollow core slabs were developed considering material and geometrical nonlinearities, and a phased nonlinear analysis was carried out. The analytical calculations were carried out using Response-2000 program which is based on Modified Compression Field Theory (MCFT). Both the numerical and analytical models predicted the behaviour in agreement with experimental results. Parametric studies indicated that increase in the bonded overlay thickness increases the peak load capacity without reducing the displacement ductility. The increase in FRP strengthening ratio increased the capacity but reduced the displacement ductility. The hybrid strengthening technique was found to increase the capacity of the hollow core slabs by more than 100% without compromise in ductility when compared to their individual strengthening schemes.

**Keywords:** external bonding; finite element analysis; hollow core slabs; hybrid strengthening; near surface mounting; nonlinear analysis

## 1. Introduction

Prestressed hollow core slabs are precast members which are typically used as a slab and wall members in the commercial and industrial buildings, parking garages, and marine structures. Hollow core slabs typically behave as simply supported one way slabs and provides longer clear span when compared to conventional reinforced concrete slabs. Strengthening of these hollow core slabs is required for several reasons, such as to maintain the structural integrity, change in loads, and provision of openings for service utilities (Pachalla and Prakash 2017). In the past, many of researchers (Walraven and Mercx 1983, Becker and Buettner 1985, Pajari 1998, Hawkins and Ghosh 2006, Palmer and Schultz 2011) have studied the flexural and shear behaviour of hollow core slabs by considering various parameters such as shear span to depth ratio, prestressing force, depth of the slab, and cross sectionalshape of the slabs. Many previous works have focused on using Fiber reinforced polymers (FRP) for strengthening of RC beams and prestressed concrete (PSC) beams (El-Hacha and Rizkalla 2004, Hawileh 2012, Panda *et al.* 2013, Sakar *et al.* 2014, Sharaky *et al.* 2014, Ghasemi *et al.* 2015, Saribiyik and Caglar 2016). However, only a handful of studies are available on the behaviour of FRP strengthened hollow core slabs (Elgabbas *et al.* 2010, Pachalla and Prakash 2015, Kankeri and Prakash 2016, Pachalla and Prakash 2017).

Moreover, the effect of different strengthening techniques on the behaviour of hollow core slabs has not been fully investigated and understood. Barbosa and Riberio (1998) carried out finite element analysis of RC beams using commercial FE software ANSYS. The authors found that the non-linear stress-strain curve of concrete under compression plays a major role in predicting the accurate behaviour of the beams. Wang (2007) carried out the FE analysis of hollow core slabs to predict the shear capacity and concluded that the service load capacity from FE analysis matched well with experimental values. Hegger *et al.* (2010) performed the finite element analysis of hollow core slabs on different support conditions. They observed that the initial stiffness and shear deformation was captured very well by finite element model. Pachalla and Prakash (2017) carried out finite element analysis of FRP strengthened hollow core slabs with openings. They found that the FE models were able to predict the behaviour of prestressed hollow core slabs reasonably well with peak load predictions differing by an average of 4%. The existing literature studies (Yang 1994, Lam *et al.* 2000, Brunesi *et al.* 2014, Brunesi and Nascimbene 2015) indicates that the

*Corresponding author, Associate Professor
E-mail: suriyap@iith.ac.in
[a]Ph.D. Scholar
E-mail: ce14resch01002@iith.ac.in
[b]Assistant Professor
E-mail: sameer.pachalla@mechyd.ac.in



ISSN: 1225-4568 (Print), 1598-6217 (Online)

nonlinear finite element models developed can predict the behaviour of prestressed hollow core slabs reasonably well can be used for carrying out parametric studies and develop design guidelines.

## 2. Research significance and objectives

The review of studies carried out in the past clearly indicates that only a handful of studies were available on the FE modelling of FRP strengthened hollow core slabs under flexure and shear. The scope of this study is to (i) develop finite element models of hollow core slabs with different strengthening techniques and validate it with the experimental results, (ii) carry out parametric studies to understand the influence of various parameters like FRP reinforcement ratio, thickness of bonded overlay and their hybrid strengthening combinations, (iii) analyse the strengthened hollow core slabs using MCFT based Response 2000 program. The commercial finite element software ANSYS is used to model the behaviour of hollow core slabs with actual geometry and boundary conditions as used in the experimental study (Kankeri and Prakash 2017). Two shear span to depth (a/d) ratios of 3.75 and 7.50 were chosen to replicate the previous experimental study of the authors. The behaviour of hollow core slabs were also analytically predicted using Response 2000. Response 2000 is a program developed at University of Toronto based on modified compression field theory (MCFT) (Bentz *et al.* 2006). Both the analytical and FE results were used to understand the effect of a/d ratio on the efficiency of different strengthening techniques.

## 3. Experimental program

### *3.1 Overview*

The detailed information of the experimental program is not mentioned in this paper and it can be found elsewhere (Kankeri and Prakash 2017). However, an overview of the test program is briefly mentioned here for better understanding of the finite element modelling considered in this study. A total of twelve full-scale hollow core slabs were tested under two different shear span to depth (a/d) ratios of 3.75 and 7.5 to understand shear and flexure dominated failure modes, respectively. The dimensions of slabs used for investigation are 600 mm in width, 150 mm in depth and 3500 mm in length (Fig. 1). The schematic front and the plan view of the experimental test setup is illustrated in Fig. 1. All the hollow core slabs were cast using normal weight ready mix concrete to have a target cubic compressive strength of 40 MPa at 28 days. The average compressive strength of the cube after 28 days of curing was 43 MPa. To ensure monolithic behaviour, the average compressive strength of hollow core slab and bonded overlay were kept nearly same. Cubes were cast while preparing bonded overlay strengthening of hollow core slabs. The average cubic compressive strength was found to be 37 MPa.

The sectional details of different strengthening schemes

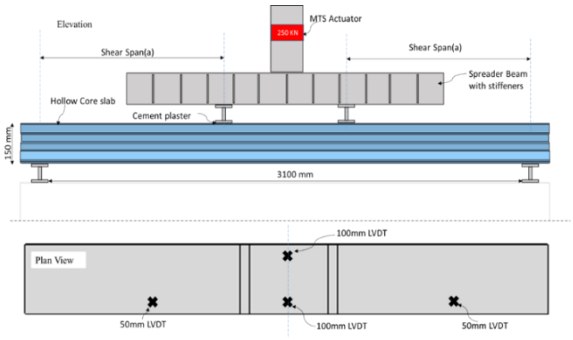


Fig. 1 Schematic of test setup

Table 1 Specimen details

| S. No | Nomenclature | a/d ratio | Strengthening details |
|---|---|---|---|
| 1 | 7.5-C | 7.50 (series I) | Control slab |
| 2 | 7.5-BO | | Bonded Overlay |
| 3 | 7.5- NSM | | CFRP NSM |
| 4 | 7.5- EB | | externally bonded with CFRP |
| 5 | 7.5- HYB-NSM | | Hybrid- bonded overlay with CFRP NSM |
| 6 | 7.5- HYB-EB | | Hybrid- Bonded overlay with CFRP EB |
| 7 | 3.75- C | 3.75 (series II) | Control Slab |
| 8 | 3.75-BO | | Bonded Overlay |
| 9 | 3.75- NSM | | CFRP NSM |
| 10 | 3.75- EB | | CFRP externally bonded |
| 11 | 3.75- HYB-NSM | | Hybrid- bonded overlay with CFRP NSM |
| 12 | 3.75- HYB-EB | | Hybrid- bonded overlay with CFRP EB |

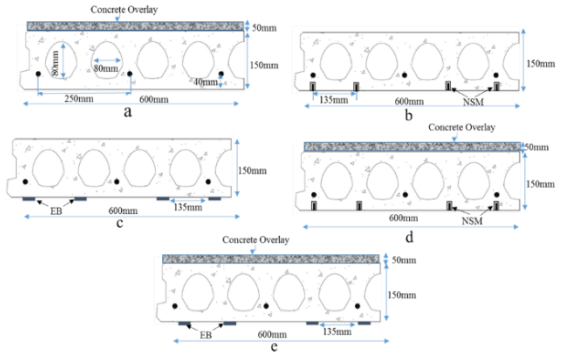


Fig. 2 Cross section details (a) HCS+BO (b) HCS+NSM (c) HCS+EB (d) HCS+BO+NSM and (e) HCS+BO+EB

Table 2 CFRP laminate properties

| Material | Dimensions (mm) | Ultimate elongation (%) | Tensile strength (MPa) | Modulus of elasticity (GPa) |
|---|---|---|---|---|
| CFRP | 25 x 1.4 | 1.3 | 2300 | 150 |

considered in the study are shown in Fig. 2. Similarly, the nomenclature of the specimens is given in Table 1. The slabs were divided into two series viz. I and II based on the a/d ratio. Strengthening of these slabs by EB and NSM techniques was done using CFRP laminates. The properties of CFRP laminates were evaluated using coupon test and are shown in Table 2.


(a) Externally bonded CFRP laminates


(b) NSM CFRP strengthened HCS

Fig. 3 EB and NSM strengthened specimens


(a) Installation of shear keys


(b) NSM CFRP strengthened HCS

Fig. 4 Provision of shear keys at the interface of parent slab and bonded overlay

### 3.2 Strengthening procedure

#### 3.2.1 EB and NSM strengthening

Fig. 3 shows the hollow core slabs strengthened with CFRP laminates. For the NSM strengthening, CFRP laminates were inserted into the grooves made at the bottom of the slab. The grooves were prepared as per ACI 440.2R guidelines. Strengthening of hollow core slabs by external bonding (EB) technique was done by fixing CFRP laminates at the bottom of the slab using epoxy resin. The laminates were of 25 mm wide and 1.4 mm thick in both the techniques. Detailed strengthening procedures can be found elsewhere (Kankeri and Prakash 2017).

#### 3.2.2 Strengthening with bonded overlay

A 50 mm thick concrete overlay was placed in the compression zone of the slab. To ensure the monolithic behaviour of hollow core slab and bonded overlay throughout the testing a minimum number of shear keys were provided as per ACI 318. Fig. 4 shows the placing of shear keys. L-shaped shear keys made up of 8 mm diameter bars were placed at 300 mm c/c along the length of the hollow core slab and 250 mm c/c along the width. These slabs were tested after 28 days curing of bonded overlay concrete.


(a) Placing of LVDT's

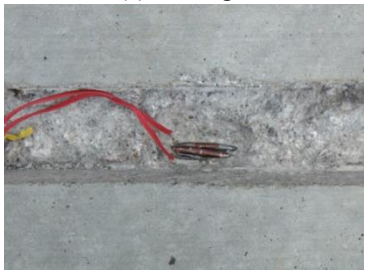
(b) Installation of strain gauge on strands

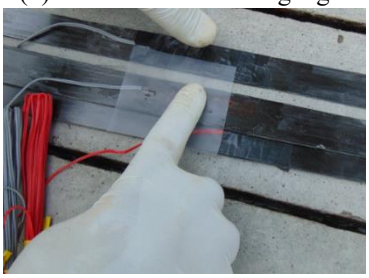
(c) Installation of strain gauges on laminates

Fig. 5 Placing of LVDT's and strain gauges

### 3.3 Test details

A 250 kN hydraulic servo-controlled actuator was used to apply the load. The load was applied in the displacement control mode at a rate of 0.05 mm/sec. Loading was paused in-between to mark the cracks and observe the failure progression. To measure the displacements, Linear Variable Displacement Transducer (LVDTs) were used. Two 100 mm LVDTs were placed at the mid-span location and two 50 mm LVDTs were placed at one-third location of the span. Fig. 5(a) shows placing of LVDTs. Strain gauges with 5 mm gauge length were used to measure the strain on the strand and CFRP laminates. Fig. 5(b) and Fig. 5(c) shows the placing of strain gauges on the strand and CFRP laminates.

## 4. Finite element and analytical modelling

### 4.1 FE modelling details

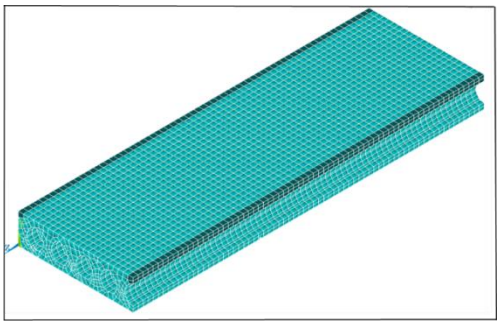

Fig. 6 Finite element (FE) model of hollow core slab using ANSYS

The commercial finite element software ANSYS 14.5 was used to develop the numerical models for all the twelve tested specimens. The geometry of the hollow core slab was modelled using CAD (computer aided design) software and was imported to the ANSYS. Due to the symmetry of these slabs along its length, only half slab was modelled to reduce the computational time. The concrete was modelled using solid 65 elements. Solid 65 is an 8 noded element with three translational degrees of freedom at each node. This element is capable of considering the plastic deformation, cracking in orthogonal directions and crushing in compression. The steel strands and CFRP laminates were modelled using a two noded LINK-180 element. Each node of this element has two translational degrees of freedom. Previous researchers (Gan 2000, Jendele and Cervenka 2006) found that the bond- slip relation between concrete and steel had minimum effect on the response of the concrete members under small deflection. Prestressing strands, CFRP laminates were modelled by assuming perfect bond with the concrete. Mesh sensitivity analysis was performed for the slabs to arrive at the optimum mesh size. Element aspect ratio of 25 mm was used for the analysis. Fig. 6 shows the isometric view of FE model of hollow core slab.

#### *4.1.1 Material models*

The Solid65 element requires linear isotropic and multilinear isotropic material properties to model the concrete behaviour in an accurate sense. The multilinear isotropic material uses the von Mises failure criterion along with the Willam and Warnke (1974) model to define the failure of the concrete. $E_X$ is the modulus of elasticity of the concrete ($E_c$) based on the Eq. 1. The developed FE models had similar material properties of the actual tested specimens. Concrete cylinders were tested in the laboratory to obtain the strength of concrete on the date of testing. Average cylinder strength of concrete was found to be 34 MPa. The elastic modulus and Poisson's ratio of concrete were taken as 33200 MPa and 0.2, respectively. Nonlinear stress strainbehaviour of concrete under compression was modelled using Hognestad (1951) model and the governing equation is shown in Eq. (2). The stress strain curve of prestressing strands was modelled by the equation proposed by Ramberg and Osgood (1943) with initial elastic modulus and Poisson's ratio as 196.5 GPa and 0.3, respectively. Prestressing strands do not have a well-defined yield point

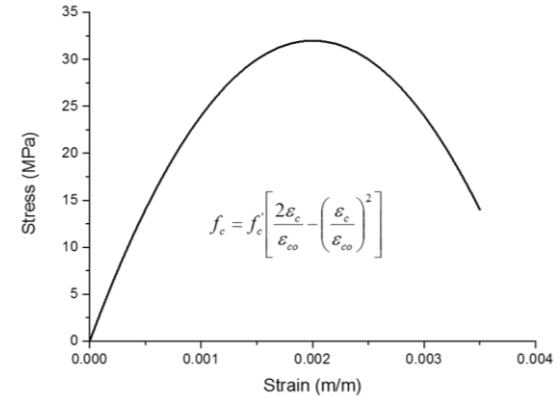


(a) Concrete in Compression

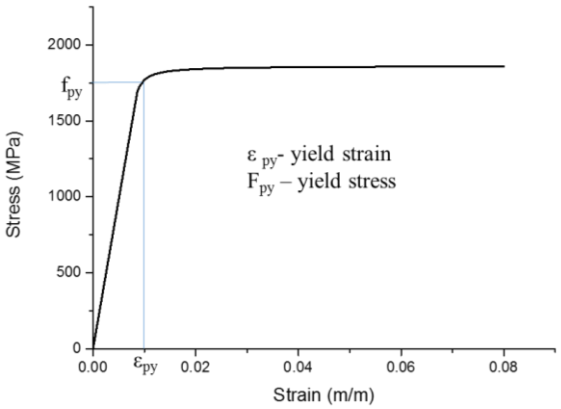


(b) Prestressing strands

Fig. 7 Material inputs-stress strain curve

and therefore, a value of 10,000 $\mu$m/m is taken as yielding strain (Devalapura and Tadros 1992). The corresponding yield stress is taken as 1680 MPa.

$$E_c = 5700\sqrt{f'_c} \tag{1}$$

$$f_c = f_c'\left[\frac{2\varepsilon_c}{\varepsilon_{co}} - \left(\frac{\varepsilon_c}{\varepsilon_{co}}\right)^2\right] : \text{for } 0 \le \varepsilon_c \le \varepsilon_{co} \tag{2}$$

where $f_c$ = concrete compressive stress (MPa), $f_c'$ = concrete cylinder compressive strength (MPa), $\varepsilon_c$ = concrete strain, $\varepsilon_{co}$ = concrete strain corresponding to $f_c'$, $E_c$ = Young's modulus of concrete (MPa) and $\varepsilon_{co} = \frac{2 * f'_c}{E_c}$. (3)

#### *4.1.2 Loading and boundary conditions*

To model the accurate behaviour, care must be taken to simulate the boundary conditions in FE models similar to the experiments. The bottom nodes on the left end of the slabs were pinned with restraints in the vertical direction. Symmetric boundary conditions were applied to the area at the right end of the model. Vertical displacement was applied at the top surface nodes at a distance from supports calculated based on the chosen shear span to depth (a/d)

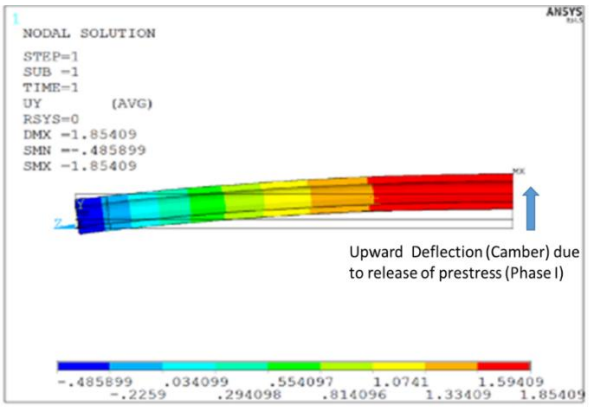


(a) Phase I

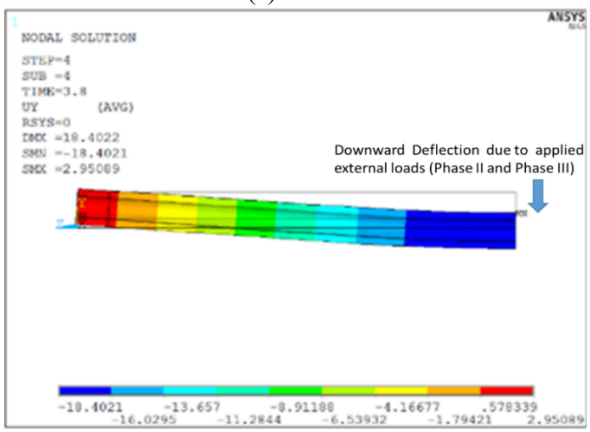


(b)Phase II and III

Fig. 8 Deflection of slabs in phased analysis

ratio. Downward displacement was applied to the full line of nodes until the complete failure of the slab. The displacement was increased in small increments after cracking to avoid the convergence difficulties.

#### *4.1.3 Phased analysis*

The analysis was carried out in three phases and at each phase the results of previous phase act as input for subsequent phases. Before carrying out the phased analysis, all the elements such as concrete, steel, CFRP reinforcement and bonded overlay were modelled. In the first phase, the prestressing force was applied to the strands by using INISTATE command. In this phase, the CFRP laminates and bonded overlay concrete were de-activated by using EKILL command. After releasing of strands, prestressing force creates upward deflection (camber) in the slab which is showed in Fig. 8(a). In the second phase, the deactivated elements were activated using EALIVE command. In the third phase, downward displacement was applied on the top surface nodes at a distance from support nodes as per the a/d ratio. The downward displacement of the slab shown in Fig. 8(b). Incremental displacement was applied on these selected nodes. The analysis was stopped when convergence criteria were not met in the analysis or strain in the FRP reached its rupture strain. The displacement convergence tolerance of 0.05 was used in this study. The total vertical reaction was calculated by multiplying the reaction of left side support nodes by two.

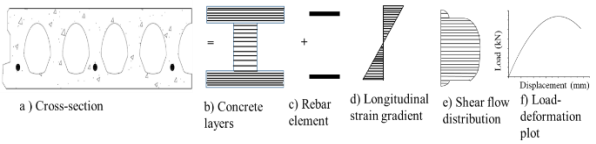


Fig. 9 Hollow core slab sectional analysis using layer by layer model

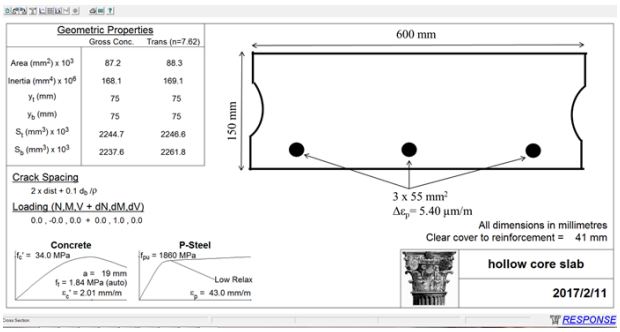


Fig. 10 Cross section details of hollow core slab specified in the Response-2000

The total reaction was plotted against the vertical deflection of the mid-span nodes to generate the load-displacement curves.

### *4.2 Analytical modelling*

Analytical calculations were carried out using Response-2000. Response-2000 is a section level analysis program developed based on the modified compression field theory (MCFT). The MCFT employs the same set of governing equations as compression field theory (CFT), except the constitutive relationships were modified. Vecchio and Collins (1986) carried out series of experiments to calibrate the concrete stress strain in the principal compressive direction and constitutive relationship for concrete in tension. The MCFT considers the contribution of concrete in tension. The presence of principal tensile strain in the concrete decreases the principal compressive strength of concrete.

Response-2000 treats hollow core slab into equivalent I-section, composed series of concrete and reinforcement elements as shown in Fig. 9(b) and Fig. 9(c), respectively. Each cross section is treated as a stack of biaxial elements and the concrete layer and steel elements are analyzed individually though the condition of equilibrium and compatibility should be satisfied for the section as a whole. For analytical calculation, the longitudinal strain and shear flow distribution across the section were assumed as shown in Fig. 9(d) and Fig. 9(f), respectively. Each concrete element and rebar element analyzed separately. The longitudinal stress in the rebars can be calculated directly from assumed longitudinal strain. The calculation of longitudinal stress in the concrete element is slightly difficult. However, for assumed longitudinal strain and normal shear stress acting on the particular concrete element, the remaining stress and strain can be found by using modified compression field theory formulations. Thus, for assumed longitudinal strain and shear flow, the

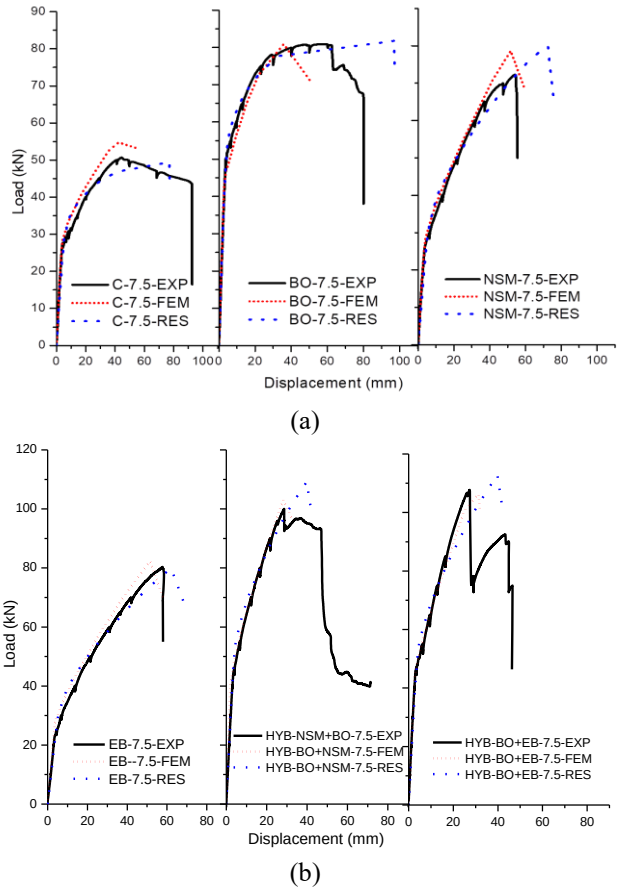


Fig. 11 Load- Displacement comparison for slabs in series I

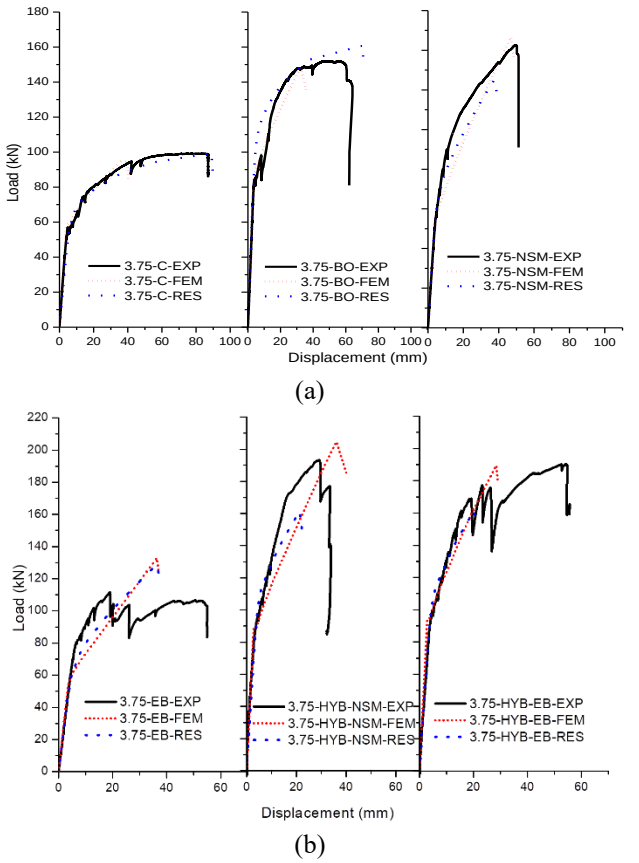


Fig. 12 Load-Displacement comparison for slabs in series II

longitudinal stress can be calculated for each concrete and steel elements. The resultant of these stress must balance the applied sectional forces. If these conditions are not satisfied, then it becomes necessary to re-assume the longitudinal strain gradient and shear flow. Response 2000 is a two-dimensional sectional analysis program predicts the complete load-deformation of reinforced and prestressed concrete beams under combined flexure and shear. Moreover, Response-2000 also has a special provision for predicting the load-deformation of hollow core slabs. The cross-section details and material properties are provided as input to the Response-2000. For externally bonded and NSM strengthened specimens, the CFRP laminates were modelled as external longitudinal reinforcement with appropriate material properties obtained from the coupon tests. Similarly, additional overlay in the bonded overlay specimen was assumed to be monolithic with that of parent slab as no interfacial failures were observed in the experiments. Fig. 10 shows the cross-sectional details provided for the hollow core slab in Response-2000.

## 5. Results and discussion

### *5.1 Comparison of load – displacement behaviour*

The load- displacement curves obtained from FE and analytical models are compared with experimental results in Figs. 11 and 12. Mid span deflection of tested slabs is measured using LVDTs and is plotted against the applied actuator load to get the experimental load-displacement response of the slabs. Similarly, the top node deflection at the mid span location was plotted against the vertical reaction forces at the supports in finite element models.

#### *5.1.1 Series I (a/d ratio 7.5)*

The load - displacement response of all the six slabs tested in series-I are compared in Fig. 11. The slabs were tested at an a/d ratio 7.5 to simulate a flexure dominant behaviour. The specimen without strengthening (7.5- C) served as control specimen for this series. The control slab had the first crack in the mid-span location at a load of 25 kN. Further increase in applied load resulted in more distributed cracks in the constant moment zone. A peak load of 50.7 kN was reached after considerable yielding of strands. The specimen finally failed due to the crushing of concrete in compression. The finite element model also exhibited a similar cracking behaviour as observed in the experiments. The pre and post-cracking stiffness of FE model matched closely with the test result. It had a peak load of 52 kN with an error less than 5% when comparison with the experiments. Specimen strengthened with only bonded overlay (7.5-BO) technique experienced a peak load of 78.9 kN with a mid-span deflection of 52.6 mm. The bonded overlay specimen increased the strength by 57.2% compared to the control slabs without compromising the ductility. The finite element model of bonded overly slab predicted a peak load of 80.9 kN which was closely

matching with the experimental result. Under-reinforced failure mode was observed in both experiment and FE model.

The experimental response of both externally bonded (7.5-EB) and NSM strengthened (7.5-NSM) specimens had the same pre-cracking and post-cracking stiffness. For these specimens, the experimental peak loads were 80.3 kN and 72.3 kN, respectively. The FE models predicted the peak load of 82 kN and 78 kN indicating again a close correlation with the test results. The experimental response of hybrid strengthened specimen with external bonding (7.5-HYB-EB-EXP) had an initial flexural crack in the constant moment zone at a load of 45 kN. At higher loads, a sudden drop in the load was observed at a load of 107 kN due to local debonding of the laminate and the slab failed in the flexure-shear mode. The finite element model of the externally bonded hybrid strengthened specimen (7.5-HYB-EB-FEM) accurately predicted the overall load displacement behaviour and peak load. Similarly, the finite element model of NSM hybrid strengthened specimen (7.5-HYB-NSM-FEM) predicted the pre-cracking and post-cracking behaviour accurately. Table 3 summarizes the comparison of experimental and FE results of this series. Fig. 11 clearly indicates that Response-2000 is able to closely predict the cracking and peak loads for control specimen. Similarly, for all other tested specimens, the Response-2000 accurately predicted the cracking load, initial stiffness, post cracking stiffness and peak load (Table 3).

Table 3 Comparison of experimental and numerical results

| Specimen | Exp. cracking load (kN) | FE cracking load (kN) | Cracking load predicted by Response-2000 (kN) | Experimental peak load (kN) | Peak load Predicted by FE (kN) | Peak load predicted by Response-2000 (kN) | $P_{FEM}/P_{EXP}$ | $P_{RES}/P_{EXP}$ |
|---|---|---|---|---|---|---|---|---|
| 7.5-C | 25.0 | 26.0 | 26.0 | 50.7 | 52.0 | 49.4 | 1.02 | 0.97 |
| 7.5-BO | 50.2 | 42.7 | 53.1 | 78.9 | 80.9 | 81.7 | 1.02 | 1.03 |
| 7.5-NSM | 28.5 | 29.0 | 30.0 | 72.3 | 78.0 | 80.0 | 1.07 | 1.10 |
| 7.5-EB | 28.0 | 29.0 | 30.0 | 80.3 | 82.0 | 79.9 | 1.02 | 0.99 |
| 7.5-HYB-NSM | 42.2 | 43.0 | 48.0 | 100.0 | 103.0 | 109.1 | 1.03 | 1.09 |
| 7.5-HYB-EB | 45.0 | 43.0 | 50.0 | 107.7 | 106.3 | 112.8 | 0.98 | 1.04 |
| 3.75-C | 57.0 | 58.0 | 57.5 | 95.5 | 94.7 | 99.3 | 0.99 | 1.03 |
| 3.75-BO | 82.0 | 82.0 | 95.0 | 152.0 | 148.0 | 160.7 | 0.97 | 1.05 |
| 3.75-NSM | 58.0 | 59.0 | 59.0 | 142.7 | 146.6 | 126.8 | 1.03 | 0.88 |
| 3.75-EB | 78.0 | 60.0 | 60.0 | 111.7 | 124.5 | 129.9 | 1.11 | 1.16 |
| 3.75-HYB-NSM | 95.0 | 94.8 | 96.0 | 193.0 | 191.6 | 161.5 | 0.99 | 0.83 |
| 3.75-HYB-EB | 95.0 | 95.0 | 97.0 | 190.5 | 189.6 | 161.3 | 0.99 | 0.85 |

### *5.1.2 Series II (a/d ratio 3.75)*

The load v/s displacement response of the all six slabs tested in series II (low a/d =3.75) is shown in Fig. 12. The experimental response of control slab (3.75-C) had a linear behaviour until the first crack appeared at a load of 57 kN. The slab had a peak load of 95.5 kN and failed by concrete crushing after the yielding of prestressing strands. Cracking load of 58 kN was observed in FE predictions. The pre-cracking stiffness of FE result was similar to that of experimental response. After first cracking, the change in stiffness was accurately captured in FE model. The FE analysis resulted in the peak load of 94.7 kN which matched closely with the test result. The slab strengthened with bonded overlay (3.75-BO) had a first crack below the loading point at a load of 82 kN. The slab resisted a peak load of 152 kN with the corresponding displacement of 49.9 mm before failing in diagonal shear-tension. The slab strengthened with bonded overlay showed an increase in strength of about 60% when compared to the control slab. The finite model of this specimen predicted the cracking load 82 kN and peak load of 148 kN. The pre-cracking response, cracking load and peak load was accurately captured by FE model. The diagonal shear crack pattern in FE model also matched with the test result. The specimen strengthened with externally bonded CFRP laminates (3.75-EB) had a cracking load of 78 kN and a peak load of 111.7 kN. After reaching peak load, multiple local debonding failures were observed in the shear zone and slab finally failed in shear tension mode due to local FRP debonding. The finite element model of this specimen predicted a cracking load of 60 kN and peak load of 124.5 kN.

The experimental response of the specimen strengthened with NSM CFRP laminates (3.75- NSM) had the initial crack at the load of 58 kN. With further increase in load, a diagonal crack formed in the shear region and the slab failed in shear tension at a peak load of 142.7 kN. The finite element model also had a similar pre-cracking stiffness with a slight deviation in the post-cracking response when compared with the experimental response. However, the FE model of NSM strengthened specimen predicted the peak load accurately. The experimental response of hybrid externally bonded strengthened specimen (3.75- HYB-EB) had a linear behaviour until the first cracking at a load of 95 kN. Multiple load drops were observed (Fig. 12) due to progressive debonding of externally bonded CFRP laminates. This slab resisted a peak load of 190.5 kN before failing suddenly in shear tension mode. The FE model of this specimen predicted the pre-cracking stiffness and cracking load closely. The peak loads also matched very well. The hybrid NSM strengthened specimen (3.75-HYB-NSM) had a similar failure progression as that of specimen strengthened with hybrid externally bonded laminates. The experimental cracking and peak loads were 95 kN and 193 kN, respectively. The finite element model of this specimen accurately predicted the cracking load and pre-cracking stiffness. A deviation of about 5% was observed in peak load prediction when compared to the experimental values.

Fig. 12 shows the load - displacement for slabs tested under low shear span to depth ratio of 3.75. For control slab and slab strengthened with bonded overlay, the Response-2000 was able to predict the cracking load, initial stiffness, and peak load very accurately. For the slab strengthened with NSM CFRP laminate, the Response-2000 was able to predict accurately the cracking load. However, it underestimates the peak load by 12.5%. Similarly, for slab strengthened with externally bonded CFRP laminates, Response-2000 over predicts the peak load by 14%. This could be due to simplification in convertingthe hollow core slab into an equivalent section. Response-2000 predicted

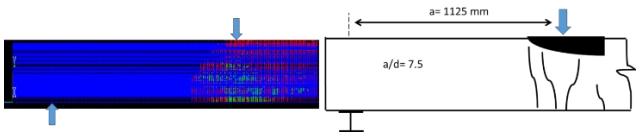


(a) Final failure of series I control specimen

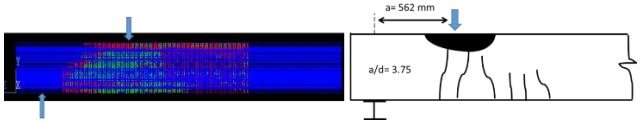


(b) Failure of series II control specimen

Fig. 13 Comparison of failure patterns

the cracking load, pre-cracking, and post-cracking stiffness accurately for the slabs strengthened with hybrid NSM and externally bonded specimens. However, the peak load for both specimens is under predicted. Table 3 summarizes all the results of specimens with numerical and analytical predictions.

### 5.2 Failure modes

The control specimen in series I, exhibited under reinforced behaviour. It failed due to the crushing of concrete in the compression zone after the yielding of prestressing strands. The slab strengthened with the bonded overlay showed the first crack in the constant moment zone and finally failed in flexure-shear. All other CFRP and hybrid strengthened specimens failed in the shear tension mode. In the control slab tested in series II, the first crack formed below the load point and more distributed cracks formed in the moment zone. The slab finally failed by crushing of concrete below the load point. For only externally bonded CFRP specimen and hybrid externally bonded specimen, the local debonding of CFRP laminates occurred in the shear zone. However, these slabs finally failed in shear tension mode. Similarly, the only NSM and hybrid NSM strengthened specimens failed in shear tension mode. This is mainly due to no appreciable increase in shear strength when compared to flexural strength improvement due to the adopted strengthening techniques.

Fig. 13(a) compares the crack progression of the FE Model and control slab of series I. This specimen had initial cracks in constant moment zone and finally failed by crushing of concrete in compression zone. The FE model also predicted the similar failure progression. Similarly, Fig. 13(b) shows the failure progression of control slab of series II. In this specimen, the first crack appeared below the load point, and more distributed cracks formed in the constant moment zone before final failure due to the crushing of concrete just below the loading point. The FE model also predicted the same failure progression. Other failure modes are not shown for brevity.

## 6. Parametric studies

Parametric studies were carried out using the calibrated models to evaluate the effect of bonded overlay thickness, FRP laminates ratio, and their hybrid strengthening schemes on the behaviour of prestressed hollow core slabs. The other parameters such as the size of the slab, prestressing force, grade of concrete and test configuration were kept the same. The first variable considered is the depth of bonded overlay. The overlay thickness is varied from 25 mm to 75 mm. To evaluate the effect of thickness of bonded overlay, two shear span to depth ratios of 3.75 and 7.5 were chosen. The FRP reinforcement ratio was considered as the second variable. The FRP reinforcement ratio ($A_f$) was varied from 0.119% to 0.478%. The variation of CFRP reinforcement

Table 4 Details of specimens and variables in parametric study

| | Specimens | Variables considered |
|---|---|---|
| Group-1 | 7.5-BO-25<br>7.5-BO-50<br>7.5-BO-75<br>3.75-BO-25<br>3.75-BO-50<br>3.75-BO-75 | Thickness of bonded overlay |
| Group-2 | 7.5-NSM-0.119<br>7.5-NSM-0.238<br>7.5-NSM-0.478<br>3.75-NSM-0.119<br>3.75-NSM-0.238<br>3.75-NSM-0.478 | % of CFRP reinforcement ratio for NSM strengthened slab |
| Group-3 | 7.5-EB-0.119<br>7.5-EB-0.238<br>7.5-EB-0.478<br>3.75-EB-0.119<br>3.75-EB-0.238<br>3.75-EB-0.478 | % of CFRP reinforcement ratio for externally bonded strengthened slab |
| Group-4 | 7.5-HYB-NSM-25-0.119<br>7.5- HYB-NSM-25-0.238<br>7.5- HYB-NSM-25-0.478<br>3.75- HYB-NSM-25-0.119<br>3.75- HYB-NSM-25-0.238<br>3.75- HYB-NSM-25-0.478 | 25 mm overlay kept constant and % of CFRP reinforcement ratio for NSM is varied |
| Group-5 | 7.5-HYB-NSM-50-0.119<br>7.5- HYB-NSM-50-0.238<br>7.5- HYB-NSM-50-0.478<br>3.75- HYB-NSM-50-0.119<br>3.75- HYB-NSM-50-0.238<br>3.75- HYB-NSM-50-0.478 | 50 mm overlay kept constant and % of CFRP reinforcement ratio for NSM is varied |
| Group-6 | 7.5-HYB-NSM-75-0.119<br>7.5- HYB-NSM-75-0.238<br>7.5- HYB-NSM-75-0.478<br>3.75- HYB-NSM-75-0.119<br>3.75- HYB-NSM-75-0.238<br>3.75- HYB-NSM-75-0.478 | 75 mm overlay kept constant and % of CFRP reinforcement ratio for NSM is varied |

Table 5 Results of parametric study

| Specimen | Cracking load (kN) | Cracking displacement (mm) | Peak load (kN) | Peak load displacement (mm) | Strength increase (%) when compared to control FE model |
|---|---|---|---|---|---|
| 7.5-C | 26.0 | 2.9 | 52 | 58.0 | -- |
| 3.75-C | 58.0 | 3.5 | 94.7 | 42.1 | -- |
| 7.5-BO-25 | 38.5 | 2.8 | 64.6 | 32.1 | 24.2 |
| 7.5-BO-50 | 42.7 | 2.8 | 80.9 | 35.8 | 55.5 |
| 7.5-BO-75 | 51.8 | 2.5 | 95.0 | 29.0 | 82.6 |
| 3.75-BO-25 | 69.9 | 2.9 | 122.4 | 33.9 | 29.3 |
| 3.75-BO-50 | 84.6 | 3.3 | 148.0 | 32.5 | 56.3 |
| 3.75-BO-75 | 108 | 2.9 | 195.9 | 41.8 | 106.8 |
| 7.5-NSM-0.119 | 23.3 | 3.0 | 76.0 | 58.3 | 46.2 |
| 7.5-NSM-0.238 | 23.0 | 2.9 | 79.0 | 49.0 | 53.0 |
| 7.5-NSM-0.478 | 23.9 | 3.0 | 96.2 | 45.0 | 85.0 |
| 3.75-NSM-0.119 | 44.3 | 2.9 | 133.6 | 57.0 | 41.1 |
| 3.75-NSM-0.238 | 44.6 | 2.9 | 143.2 | 50.0 | 51.2 |
| 3.75-NSM-0.478 | 45.3 | 2.9 | 158.9 | 42.5 | 67.7 |
| 7.5-EB-0.119 | 21.6 | 2.8 | 74.8 | 54.9 | 43.8 |
| 7.5-EB-0.238 | 21.8 | 2.8 | 82.3 | 51.4 | 58.3 |
| 7.5-EB-0.478 | 22.3 | 2.8 | 90.8 | 41.4 | 74.6 |
| 3.75-EB-0.119 | 35.2 | 2.6 | 110.6 | 46.3 | 16.7 |
| 3.75-EB-0.238 | 35.6 | 2.6 | 124.5 | 40.0 | 31.5 |
| 3.75-EB-0.478 | 36.4 | 2.6 | 142.0 | 35.3 | 49.9 |
| 7.5-HYB-NSM-25-0.119 | 34.2 | 2.8 | 96.6 | 62.5 | 85.8 |
| 7.5- HYB-NSM-25-0.238 | 34.5 | 2.8 | 114.0 | 61.7 | 119.2 |
| 7.5- HYB-NSM-25-0.478 | 35.1 | 2.8 | 133.6 | 51.4 | 156.9 |
| 7.5-HYB-NSM-50-0.119 | 44.6 | 2.8 | 103.3 | 55.5 | 98.7 |
| 7.5- HYB-NSM-50-0.238 | 45.5 | 2.8 | 125.5 | 41.7 | 141.3 |
| 7.5- HYB-NSM-50-0.478 | 47.1 | 2.9 | 147.0 | 37.0 | 182.7 |
| 7.5-HYB-NSM-75-0.119 | 51.2 | 2.5 | 143.8 | 41.9 | 176.5 |
| 7.5- HYB-NSM-75-0.238 | 52.6 | 2.5 | 163.7 | 41.5 | 214.8 |
| 7.5- HYB-NSM-75-0.478 | 54.1 | 2.5 | 175.2 | 34.7 | 237.0 |
| 3.75- HYB-NSM-25-0.119 | 62.1 | 2.9 | 168.5 | 57.2 | 77.9 |
| 3.75- HYB-NSM-25-0.238 | 62.6 | 2.9 | 184.5 | 49.0 | 94.8 |
| 3.75- HYB-NSM-25-0.478 | 63.7 | 2.9 | 198.0 | 37.7 | 109.1 |
| 3.75- HYB-NSM-50-0.119 | 92.0 | 2.6 | 204.4 | 48.1 | 115.8 |
| 3.75- HYB-NSM-50-0.238 | 92.7 | 2.6 | 224.0 | 41.8 | 136.5 |
| 3.75- HYB-NSM-50-0.478 | 93.0 | 2.7 | 240.0 | 32.7 | 153.4 |
| 3.75- HYB-NSM-75-0.119 | 105.2 | 2.6 | 270.4 | 44.3 | 185.5 |
| 3.75- HYB-NSM-75-0.238 | 112.2 | 2.6 | 289.8 | 41.9 | 206.0 |
| 3.75- HYB-NSM-75-0.478 | 114.0 | 2.6 | 317.4 | 34.8 | 235.2 |

ratio was considered for both NSM and EB techniques. Similarly, different hybrid strengthened configurations were considered by varying the overlay thickness and percentage of NSM CFRP reinforcement ratio. Table 4 summarizes the study variables and details of the specimens considered in the FE analysis. Results of the parametric studies are summarized in Table 5.

### *6.1 Effect of thickness of bonded overlay*

The thickness of the bonded overlay is varied from 25 mm to 75 mm in the group-1 models. All the slabs were analysed under at two shear span to depth ratios of 7.5 and 3.75, respectively. The increase in the thickness of the bonded overlay led to increase in cracking load, peak load and post-cracking stiffness (Fig. 14(a)).

### *6.2 Effect of NSM reinforcement ratio*

NSM CFRP reinforcement ratio is varied from 0.119% to 0.478% in group-2 models. With the increase in the longitudinal NSM ratio, post cracking stiffness and peak load increased. However, it reduced the peak load displacement and the ductility as expected due to the section becoming more over-reinforced (Fig. 14(b)). Table 5 summarizes the corresponding results of the parametric study.

### *6.3 Effect of EB reinforcement ratio*

Group-3 slabs also showed similar behaviour as that of group-2 (Fig. 14(c)). The increase in NSM laminates ratio lead to increase in the peak load without compromising the ductility. The NSM/EB CFRP strengthening increased the load capacity with an increase in the percentage of reinforcement. However, increase in the percentage of CFRP reinforcement is not always beneficial due to reduction in displacement ductility.

### *6.4 Effect of combined BO thickness and FRP reinforcement ratio*

The effect of combined bonded overlay and FRP reinforcement ratio was considered from group 4 to 6 (Figs. 14d to 14f). The overlay thickness of slab was kept constant and percentage of CFRP NSM reinforcement ratio was varied from 0.119% to 0.438%, the bonded overlay depth varied to 25 mm to 75 mm in group 4 to 6. The parametric study of hybrid strengthening indicates that simultaneous increase in the bonded overlay thickness and FRP reinforcement ratio leads to improvement in peak strength without reduction in ductility (Figs. 14(e) and 14(f)). Hence, there was an improvement in the peak load by more than 100% without compromise in ductility using this innovative hybrid strengthening scheme.

## 7. Conclusions

The effectiveness of different strengthening techniques including (i) external bonding, (ii) NSM strengthening, (iii) bonded overlay strengthening and (iv) a hybrid combination of bonded overlay and NSM/EB CFRP strengthening on the behaviour of hollow core slabs were investigated. Finite element models were developed for all the strengthening configurations. After calibrating the FE models with the experimental results, a parametric study was carried out to understand the effect of different parameters. CFRP NSM/ EB longitudinal reinforcement ratio, bonded overlay

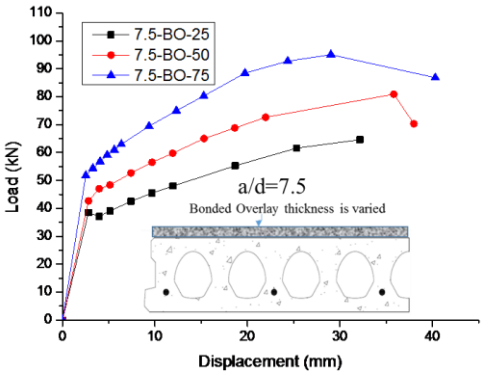


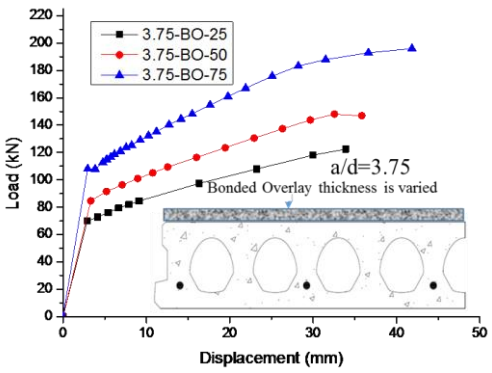


(a) Group-1

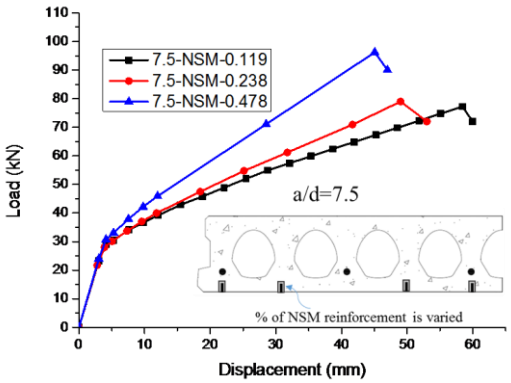


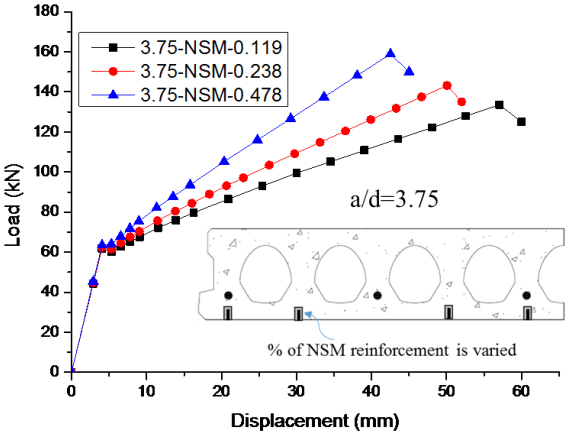


(b) Group-2

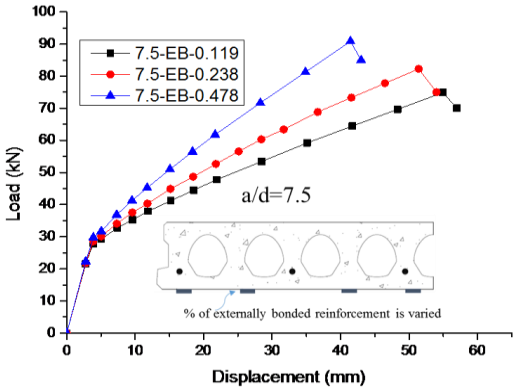


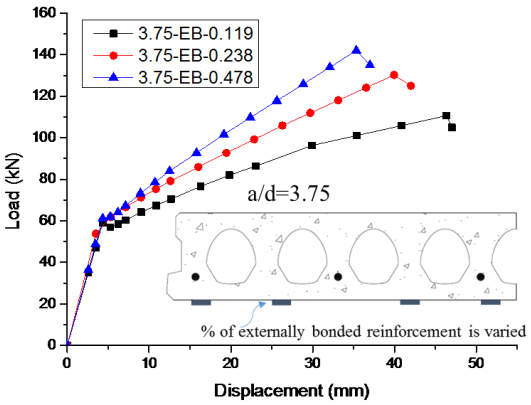


(c) Group-3

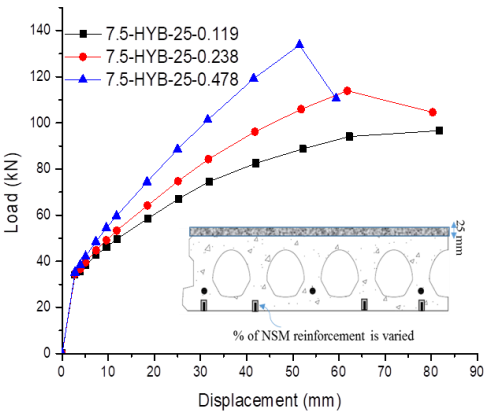


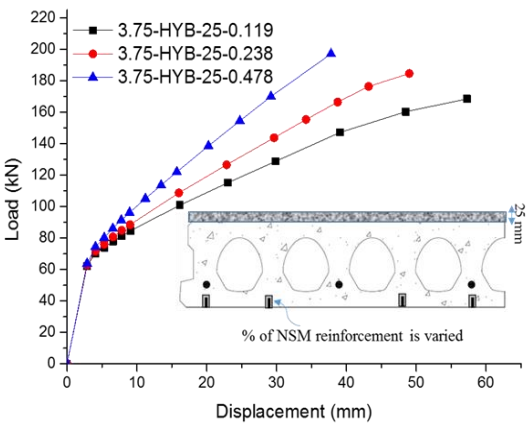


(d) Group-4

Fig. 14 Load displacementbehaviour for different parameters

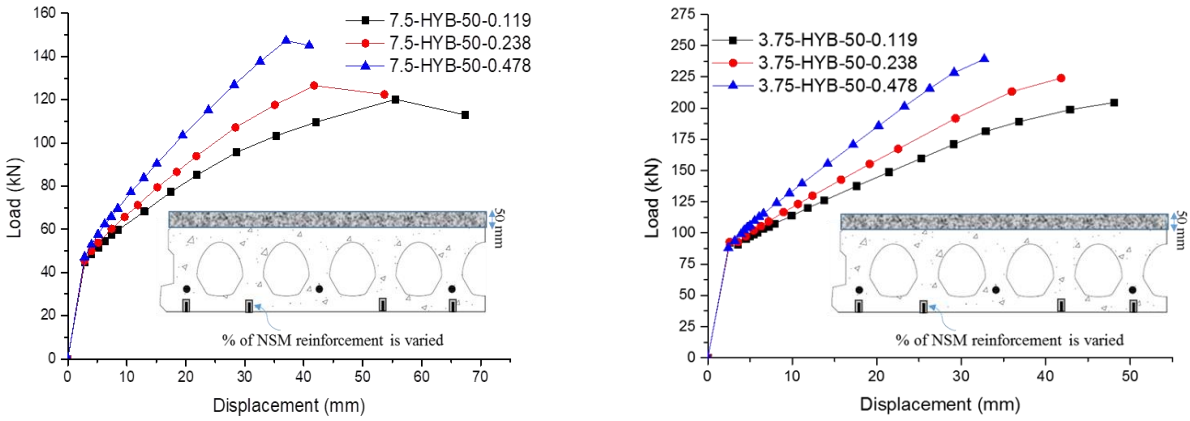


(e) Group-5

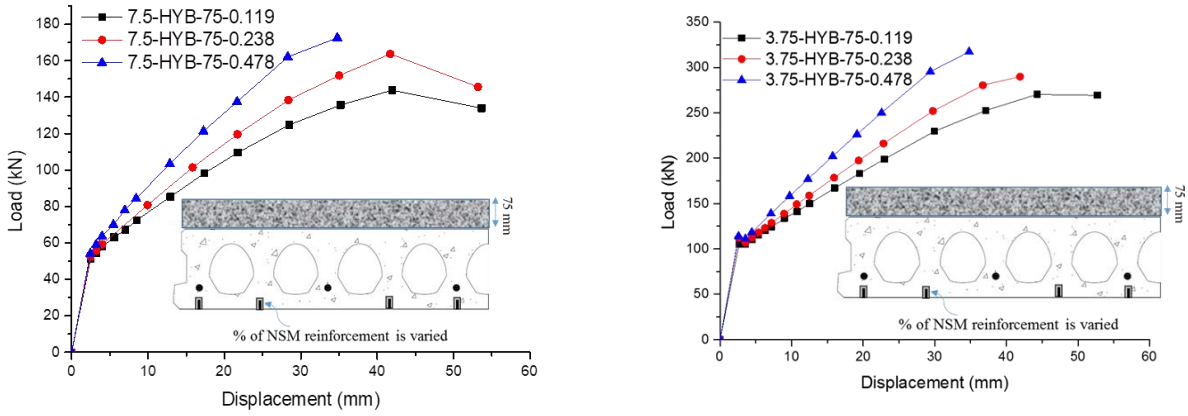


(f) Group-6

Fig. 14 Load displacementbehaviour for different parameters

thickness and their hybrid configurations were considered as the variables in the parametric study. The capacity of hollow core slabs under different strengthening techniques was also predicted analytically using Response-2000. The following are the major conclusions drawn from the results presented in this study:

• Both the numerical and analytical studies proved that hybrid strengthening could improve the performance of the prestressed hollow core slabs under both shear span to depth ratios. Significant increase in peak strength and post-cracking stiffness can be achieved by selecting a suitable bonded overlay thickness and FRP reinforcement ratio.

• The developed finite element model accurately predicted the peak strength of hollow core slabs under flexure and shear. The FE prediction of peaks loads differs by an average of 3.2% when compared to experimental results for slabs tested at both a/d ratios. Response -2000 accurately predicted the cracking load, pre-cracking and post-cracking stiffness and peak load of slabs tested at high shear span to depth ratio of 7.5 that exhibited flexure dominant behaviour. For slabs tested under low shear span to depth ratio of 3.75, the peak loads were under-predicted.

• The parametric study indicates that the increase in bonded overlay thickness lead to increase in the peak load capacity and cracking stiffness. It also indicates that the increase in FRP reinforcement ratio increases the post cracking stiffness and peak load but reduces the displacement ductility.

• The parametric study of hybrid strengthened specimens indicates that there is an optimum combination of bonded overlay thickness and NSM FRP reinforcement ratio at which the increases in peak strength by more than 100% can be achieved without much compromise in ductility.

## References

ACI 318 (2011), *Building Code Requirements for Structural Concrete and Commentary*, American Concrete Institute, Farmington Hills, MI, U.S.A.

ACI 440 (2004), *Guide for the Design and Construction of Externally Bonded FRP Systems for Strengthening Existing Structures*, American Concrete Institute, Farmington Hills, MI, U.S.A.

Barbosa, A.F. and Ribeiro, G.O. (1998), *Analysis of Reinforced Concrete Structures Using Ansys Nonlinear Concrete Model*, COMPUTATIONAL MECHANICS, New Trends and Applications S. Idelsohn, E. Oñate and E. Dvorkin (Eds.) ©CIMNE, Barcelona, Spain, 1-7.

Becker, R.J. and Buettner, D.R. (1985), "Shear tests of extruded hollow-core slabs", *PCI J.*, **30**(2), 40-54.

Bentz, E.C., Vecchio, F.J. and Collins, M.P. (2006), "Simplified modified compression field theory for calculating shear strength

of reinforced concrete elements", *ACI Struct. J.*, **103**(4), 614-624.
Brunesi, E. and Nascimbene, R. (2015), "Numerical web-shear strength assessment of precast prestressed hollow core slab units", *Eng. Struct.*, **102**, 13-30.
Brunesi, E., Bolognini, D. and Nascimbene, R. (2014), "Evaluation of the shear capacity of precast-prestressed hollow core slabs: Numerical and experimental comparisons", *Mater. Struct.*, **48**(5), 1503-1521.
Devalapura, R.K. and Tadraos, M.K. (1992), "Stress-strain modeling of 270ksi low-relaxation prestressing strands", *PCI J.*, **37**(2), 100-105.
El-Hacha, R. and Rizkalla, S.H. (2004), "Near-surface-mounted fiber-reinforced polymer reinforcements for flexural strengthening of concrete structures", *ACI Struct. J.*, **101**(5), 717-726.
Elgabbas, F., El-Ghandour, A.A., Abdelrahman, A.A. and El-Dieb, A.S. (2010), "Different cfrp strengthening techniques for prestressed hollow core concrete slabs: Experimental study and analytical investigation", *Compos. Struct.*, **92**(2), 401-411.
Gan, Y. (2000), "Bond stress and slip modelling in nonlinear finite element analysis of reinforced concrete structures", M.Sc. Dissertation, University of Toronto, Toronto, Canada.
Ghasemi, S. Maghsoudi, A.A. Bengar, H.A. and Ronagh, H.R. (2015) "Flexural strengthening of continuous unbonded post-tensioned concrete beams with end-anchored CFRP laminates", *Struct. Eng. Mech.*, **53**(6), 1083-1104.
Hawileh, R.A. (2012), "Nonlinear finite element modeling of RC beams strengthened with NSM FRP rods", *Constr. Build. Mater.*, **27**(1), 461-471.
Hawkins, N.M. and Ghosh, S.K. (2006), "Shear strength of hollow-core slabs", *PCI J.*, **51**(1), 110-114.
Hegger, J., Roggendorf, T. and Teworte, F. (2010), "FE analyses of shear-loaded hollow-core slabs on different supports", *Mag. Concrete Res.*, **62**(8), 531-541.
Jendele, J. and Cervenka, J. (2006), "Finite element modelling of reinforcement with bond", *Compos. Struct.*, **84**(28), 1780-1791.
Kankeri, P. and Prakash, S.S. (2016), "Efficient hybrid strengthening for precast hollow core slabs at low and high shear span to depth ratios", *Compos. Struct.*, **170**, 202-214.
Kankeri, P. and Prakash, S.S. (2016), "Experimental evaluation of bonded overlay and NSM GFRP bar strengthening on flexural behavior of precast prestressed hollow core slabs", *Eng. Struct.*, **120**, 49-57.
Lam, D., Elliott, K.S. and Nethercot, D.A. (2000), "Parametric study on composite steel beams with precast concrete hollow core floor slabs", *J. Constr. Steel Res.*, **54**(2), 283-304.
Pachalla, S.K.S. and Prakash, S.S. (2017), "Experimental evaluation on effect of openings on behavior of prestressed precast hollow-core slabs", *ACI Struct. J.*, **114**(2), 12.
Pachalla, S.K.S. and Prakash, S.S. (2017), "Load resistance and failure modes of GFRP composite strengthened hollow core slabs with openings", *Mater. Struct.*, **50**(3), 1-14.
Pachalla, S.K.S. and Prakash, S.S. (2018), "Load resistance and failure modes of openings-a finite element study", *PCI J.*, Accepted.
Pachalla, S.K.S. and Prakash, S.S. (2017), "Efficient near surface mounting CFRP strengthening of pretensioned hollow core slabs with opening-an experimental study", *Compos. Struct.*, **162**(2), 28-38.
Pajari, B.M. (1998), "Shear resistance of PHC slabs supported on beams. II: Analysis", *J. Struct. Eng.*, **124**(9), 1062-1073.
Palmer, K.D. and Schultz, A.E. (2012), "Experimental investigation of the web-shear strength of deep hollow-core units", *PCI J.*, **56**, 83-104.
Panda, K.C., Bhattacharyya, S.K. and Barai, S.V. (2013), "Shear strengthening effect by bonded GFRP strips and transverse steel on RC T-beams", *Struct. Eng. Mech.*, **47**(1), 75-98.
Sakar, G., Hawileh, R.A., Naser, M.Z., Abdalla, J.A. and Tanarslan, M. (2014), "Nonlinear behavior of shear deficient RC beams strengthened with near surface mounted glass fiber reinforcement under cyclic loading", *Mater. Des.*, **61**, 16-25.
Saribiyik, A. and Caglar, N. (2016), "Flexural strengthening of RC beams with low-strength concrete using GFRP and CFRP", *Struct. Eng. Mech.*, **58**(5), 825-845.
Sharaky, I. A., Torres, L., Comas, J. and Barris, C. (2014), "Flexural response of reinforced concrete (RC) beams strengthened with near surface mounted (NSM) fibre reinforced polymer (FRP) bars", *Compos. Struct.*, **109**, 8-22.
Vecchio, F.J. and Collins, M.P. (1986), "Predicting the response of reinforced concrete beams subjected to shear using modified compression field theory", *ACI Struct. J.*, **85**(3), 258-268.
Vecchio, F.J. and Collins, M.P. (1986), "The modified compression-field theory for reinforced concrete element subjected to shear", *ACI Struct. J.*, **83**(2), 219-231.
Walraven, J.C. and Mercx, W.P.M. (1983), "Bearing capacity of prestressed hollow core slabs", *Heron*, **28**, 1-46.
Wang, X. (2007) "Study on the shear behaviour of prestressed hollow core slabs by nonlinear finite element modelling", Ph.D. Dissertation, University of Windsor, Windsor, Canada.
Yang, L. (1994), "Design of prestressed hollow core slabs with reference to web shear failure", *J. Struct. Eng.*, **120**(9), 2675-2696.

*PL*